

Inelastic Diffraction and Spectroscopy of Very Weakly Bound Clusters

Martin Stoll[†] and Thorsten Köhler[‡]

[†] Institut für Theoretische Physik, Universität Göttingen, Bunsenstraße 9, 37073 Göttingen, Germany

[‡] Clarendon Laboratory, Department of Physics, University of Oxford, Oxford OX1 3PU, United Kingdom

Abstract. We study the coherent inelastic diffraction of very weakly bound two body clusters from a material transmission grating. We show that internal transitions of the clusters can lead to new separate peaks in the diffraction pattern whose angular positions determine the excitation energies. Using a quantum mechanical approach to few body scattering theory we determine the relative peak intensities for the diffraction of the van der Waals dimers $(D_2)_2$ and H_2D_2 . Based on the results for these realistic examples we discuss the possible applications and experimental challenges of this coherent inelastic diffraction technique.

PACS numbers: 36.40.-c, 03.75.Be, 34.50.Ez, 36.90.+f

1. Introduction

Since the first observation of Fresnel diffraction of atoms from a single slit in 1969 [1] diffraction of molecular beams transmitted through material devices [2, 3] has now become subject to intensive studies. New applications involve the use of transmission gratings as quantum mechanical mass spectrometers [4, 5], the determination of atomic and molecular electric dipole polarizabilities with interferometric precision [5], sensitive probing of the interaction of atoms and molecules with solid surfaces [6, 7] as well as fundamental tests of the quantum mechanical nature of complex molecules [8]. These recent developments all depend on micro-fabricated transmission gratings whose periods have now become as small as 100 nm. These small structures allow to scatter collimated molecular beams coherently. For helium beams, e.g., far more than 10 diffraction orders have been resolved whose intensities extend over more than four orders of magnitude.

With this great sensitivity diffraction from material transmission gratings can now be used for quantitative studies: Several recent experiments have shown that classical wave optics is insufficient to explain the relative magnitudes of the diffraction intensities [6, 9]. It turns out that a more general approach based on quantum mechanical scattering theory is required to include the van der Waals interaction between the atoms and the grating bars and to account for the finite size of weakly bound clusters in the beams. The

highly precise diffraction experiments together with this improved theoretical analysis have recently allowed to determine the C_3 coefficients of the atom-surface van der Waals interaction for a variety of atoms and molecules [6, 7] as well as the bond length of the helium dimer [9] which characterizes all low energy binary scattering properties of helium.

These transmission grating diffraction studies only involve elastic scattering. Atoms or molecules scattered from a solid surface can undergo internal transitions. In reflection experiments from surface lattices the coherent transfer between H_2 molecular rotational levels was observed, e.g., in reference [10]. The possibility of coherent inelastic diffraction from transmission gratings was discussed in reference [11] for the particularly interesting example of the excitation of the weakly bound helium trimer 4He_3 whose single excited state is believed to be an Efimov state (see, e.g., reference [12]). These studies have shown that, quite generally, an inelastic diffraction pattern exhibits peaks that are separated from the strong elastic diffraction maxima with an angular shift depending on the energy of the internal transition and the grating period. The principle of inelastic scattering from a material transmission grating, i.e. the (de)excitation of transmitted atoms or molecules, was demonstrated in subsequent experiments using a fine structure transition of meta-stable argon atoms [13] and a vibrational transition of meta-stable nitrogen dimers [14]. In these experimental studies, however, the transmission grating served only to multiply the intensity through the simultaneous scattering by all the parallel surfaces of the bars. The inelastic diffraction peaks implied by the periodicity of the grating have not yet been resolved.

Motivated by the recent progress in inelastic transmission scattering experiments in this article we study the coherent (de)excitation of very weakly bound two body clusters in the diffraction from a transmission grating. Based on quantum mechanical few body scattering theory we discuss to which extent the small momentum transfers that the clusters experience when they pass through the slits can excite the low energy internal transitions. We show that the small angular shifts of the inelastic diffraction peaks can be well suited to determining the transition energies. The theory is applied to the realistic examples of the van der Waals clusters $(D_2)_2$ and H_2D_2 . Their level spectra are well known both theoretically and experimentally [15, 16, 17, 18]. Furthermore, experimental beam sources for these clusters are available.

2. Diffraction of weakly bound dimers

In this section we will briefly outline the few-body scattering approach to the diffraction of weakly bound two-body systems [19] that we will apply in this article. For simplicity, we denote the two body systems as dimers although, quite generally, the constituents may be different atoms or tightly bound small molecules. These constituents are considered as point particles with masses m_1 and m_2 that interact with each other through a potential V . This potential is assumed to support shallow bound states ϕ_γ with negative binding energy E_γ .

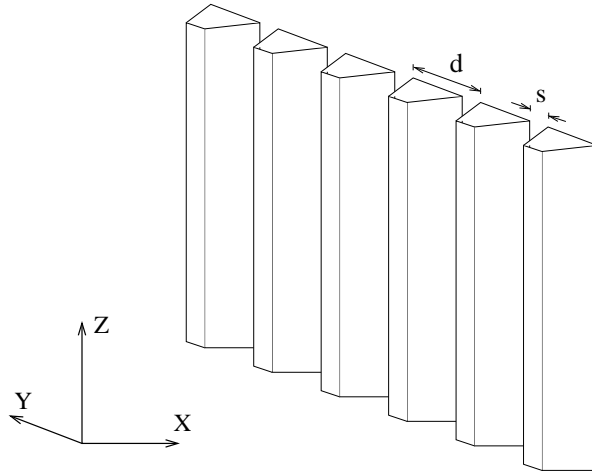


Figure 1. Scheme of the material transmission grating and the coordinate system used in this article. The bars are equally spaced with a period d . The slit width of the grating is denoted by s . The coordinates are chosen in such a way that the z direction is parallel to each bar and the grating is periodic in the y direction.

The positions of the constituents are denoted by \mathbf{x}_1 and \mathbf{x}_2 . The corresponding center of mass and relative coordinates are $\mathbf{R} = (m_1\mathbf{x}_1 + m_2\mathbf{x}_2)/(m_1 + m_2)$ and $\mathbf{r} = \mathbf{x}_1 - \mathbf{x}_2$, respectively. The diffracting object for the beam of dimers, i.e. a material transmission grating in the applications in this article, is modeled by an external potential $W(\mathbf{x}_1, \mathbf{x}_2)$. For the weakly bound dimers, under consideration, this two body potential is given, to an excellent approximation, by the sum of the potentials of each constituent, $W(\mathbf{x}_1, \mathbf{x}_2) = W_1(\mathbf{x}_1) + W_2(\mathbf{x}_2)$. With the diffraction from a transmission grating in mind we idealize the diffracting object in such a way that W is invariant with respect to translations along the z coordinate (see figure 1). This reduces the scattering problem, in the center of mass coordinates, effectively to two dimensions. The complete Hamiltonian is then given by

$$H = -\frac{\hbar^2 \nabla_{\mathbf{R}}^2}{2M} - \frac{\hbar^2 \nabla_{\mathbf{r}}^2}{2\mu} + V(\mathbf{r}) + W_1(\mathbf{x}_1) + W_2(\mathbf{x}_2), \quad (1)$$

where $M = m_1 + m_2$ and $\mu = m_1 m_2 / (m_1 + m_2)$ denote the total and reduced mass, respectively.

A beam of dimers in the state $\phi_{\gamma'}$ can be idealized as a stationary energy state of the free center of mass motion. For an incident center of mass momentum \mathbf{P}' this state is given by $|\mathbf{P}', \phi_{\gamma'}\rangle = |\mathbf{P}'\rangle |\phi_{\gamma'}\rangle$, where $|\mathbf{P}'\rangle$ is a plane wave. The total energy of a dimer in the beam then consists of the kinetic energy and the binding energy, i.e. $E' = \mathbf{P}'^2 / 2M + E_{\gamma'}$. Within the usual experimental range of (kinetic) beam energies internal excitations of the constituents should be negligible. As the dimers, under consideration, are weakly bound, however, excitations of the relative motion of their constituents as well as break-up are possible as long as the center of mass kinetic energy exceeds the dissociation threshold. We will study in this article the (de)excitation of dimers from the bound state $\phi_{\gamma'}$ to ϕ_{γ} at beam energies that are large in comparison

to the break-up threshold. We will thus assume

$$|E_0| \ll (P_x'^2 + P_y'^2)/2M, \quad (2)$$

where E_0 is the ground state binding energy of the dimer. We shall further presuppose the diffraction condition, i.e. we assume that the de Broglie wave length of an incoming dimer, $\lambda' = 2\pi\hbar/P'$, is by far smaller than all length scales set by the diffracting object. The characteristic length scales of a transmission grating are the slit width s and the width of the bars $d - s$ (see figure 1). Under typical experimental conditions the ratios s/λ' and $(d - s)/\lambda'$ are of the order of several hundreds or larger. The diffraction condition assures that the outgoing intensity is sharply peaked about the incident beam direction with a typical width of several mrad.

The scattering matrix, S , maps the incoming state $|\mathbf{P}', \phi_{\gamma'}\rangle$ onto the outgoing state, i.e. the asymptotic state after the diffraction from the potential W . The S matrix element that describes the (de)excitation of a dimer can be decomposed as

$$\begin{aligned} \langle \mathbf{P}, \phi_\gamma | S | \mathbf{P}', \phi_{\gamma'} \rangle &= \delta^{(3)}(\mathbf{P} - \mathbf{P}') \delta_{\gamma\gamma'} - 2\pi i \delta(E - E') \delta(P_z - P_z') \\ &\times t(P_x, P_y, \phi_\gamma; P_x', P_y', \phi_{\gamma'}), \end{aligned} \quad (3)$$

where $E = \mathbf{P}^2/2M + E_\gamma$ is the energy of the outgoing dimer. In reference [19] the dimer transition amplitude $t(P_x, P_y, \phi_\gamma; P_x', P_y', \phi_{\gamma'})$ has been determined from a general approach to few-body multi-channel scattering theory [20], by means of perturbation theory. According to this approach the dimer transition amplitude can be expressed in terms of ‘‘point particle’’ transition amplitudes of the constituents:

$$t_i^{\text{PP}}(p_{ix}, p_{iy}; \Delta p_{ix}, \Delta p_{iy}) = \langle p_{ix}, p_{iy} | W_i | p'_{ix}, p'_{iy}, + \rangle_i. \quad (4)$$

Here p'_{ik} and p_{ik} , $i = 1, 2$, $k = x, y$ denote the momentum components of a single constituent and $\Delta p_{ik} = p_{ik} - p'_{ik}$ the corresponding momentum transfers. Furthermore, $|p'_{ix}, p'_{iy}, +\rangle_i$ is the stationary outgoing scattering state that corresponds to the diffraction of constituent i with incident momentum (p'_{ix}, p'_{iy}) from the potential W_i [19]. From reference [19] one then obtains

$$\begin{aligned} t(P_x, P_y, \phi_\gamma; P_x', P_y', \phi_{\gamma'}) &= t_1^{\text{PP}} \left(\frac{m_1}{M} P_x, \frac{m_1}{M} P_y; \Delta P_x, \Delta P_y \right) F_{\gamma\gamma'} \left(-\frac{m_2}{M} \Delta \mathbf{P} \right) \\ &+ t_2^{\text{PP}} \left(\frac{m_2}{M} P_x, \frac{m_2}{M} P_y; \Delta P_x, \Delta P_y \right) F_{\gamma\gamma'} \left(\frac{m_1}{M} \Delta \mathbf{P} \right) \\ &- \frac{2\pi i M}{P_x} \int dq_y t_1^{\text{PP}} \left(\frac{m_1}{M} P_x, \frac{m_1}{M} P_y; \Delta P_x, \frac{m_1}{M} \Delta P_y - q_y \right) \\ &\times t_2^{\text{PP}} \left(\frac{m_2}{M} P_x, \frac{m_2}{M} P_y; 0, \frac{m_2}{M} \Delta P_y + q_y \right) F_{\gamma\gamma'} \left(-\frac{m_2}{M} \Delta P_x, q_y, 0 \right), \end{aligned} \quad (5)$$

where

$$F_{\gamma\gamma'}(\mathbf{p}) = \int d^3r \exp(-i\mathbf{p} \cdot \mathbf{r}/\hbar) \phi_\gamma^*(\mathbf{r}) \phi_{\gamma'}(\mathbf{r}) \quad (6)$$

is usually referred to as the form factor of the dimer that corresponds to the transition from $\phi_{\gamma'}$ to ϕ_γ .

In reference [21] the transition amplitude (4) has been expressed in terms of a Fourier transform of a point particle transmission function τ_i^{PP} , $i = 1, 2$ (see Appendix):

$$t_i^{\text{PP}}(p_{ix}, p_{iy}; \Delta p_{ix}, \Delta p_{iy}) = -i \frac{p_{ix}}{(2\pi)^2 m_i \hbar} \times \int dy \exp(-i\Delta p_{iy}y/\hbar) \left[1 - \tau_i^{\text{PP}}(p'_{ix}, p'_{iy}; y) \right]. \quad (7)$$

This representation is particularly useful in the description of diffraction scattering close to the incident beam direction. If, for instance, the interaction of the constituents with the grating bars is assumed to be purely repulsive τ_i^{PP} recovers the grating transmission function of classical optics and equation (7) becomes the classical Kirchhoff diffraction amplitude [22, chap. 8.5].

We shall use equation (7) to represent the dimer transition amplitude (5) in terms of a dimer transmission function: Inserting equation (7) into equation (5) and performing the momentum integrals shows that, under the diffraction condition and within the range of validity of assumption (2), some terms in equation (5) cancel. The dimer transition amplitude then assumes the form:

$$t(P_x, P_y, \phi_\gamma; P'_x, P'_y, \phi_{\gamma'}) = -i \frac{P_x}{(2\pi)^2 M \hbar} \times \int dY \exp(-i\Delta P_y Y/\hbar) \left[\delta_{\gamma\gamma'} - \tau_{\gamma\gamma'}^{\text{dim}}(P'_x, P'_y; Y) \right], \quad (8)$$

where the dimer transmission function is given by

$$\tau_{\gamma\gamma'}^{\text{dim}}(P'_x, P'_y; Y) = \int d^3r \phi_\gamma^*(\mathbf{r}) \phi_{\gamma'}(\mathbf{r}) \times \tau_1^{\text{PP}} \left(\frac{m_1}{M} P'_x, \frac{m_1}{M} P'_y; Y + \frac{m_2}{M} y \right) \tau_2^{\text{PP}} \left(\frac{m_2}{M} P'_x, \frac{m_2}{M} P'_y; Y - \frac{m_1}{M} y \right). \quad (9)$$

The coordinates $\mathbf{R} = (X, Y, Z)$ and $\mathbf{r} = (x, y, z)$ in equation (9) can be interpreted as center of mass and relative coordinates, respectively.

3. Diffraction from a Transmission Grating

In this section we will analyze the kinematic diffraction phenomena that are implied by the periodicity of a material diffraction grating consisting of equally spaced bars with a period d and a slit width s (see figure 1). The grating potential of each constituent is assumed to be strongly repulsive inside the bars with an attractive part along their surfaces that accounts for the van der Waals interaction of the constituents with the material [6]. The periodicity of the grating along the y axis reappears in the point particle transmission functions τ_i^{PP} and thus, by equation (9), the dimer transmission function $\tau_{\gamma\gamma'}^{\text{dim}}$ is also periodic in the center of mass coordinate Y . As a short calculation using equation (9) shows, this periodicity implies the conservation of the y component of the center of mass momentum of a dimer, up to reciprocal lattice vectors \ddagger :

$$\Delta P_y = n2\pi\hbar/d, \quad n = 0, \pm 1, \pm 2, \dots \quad (10)$$

\ddagger This conservation law can also be deduced from general symmetry considerations.

Furthermore, the conservation of the total energy and the translational invariance of the grating along the z axis imply

$$(P_x'^2 + P_y'^2)/2M + E_{\gamma'} = (P_x^2 + P_y^2)/2M + E_{\gamma}. \quad (11)$$

These conservation laws determine, in turn, the angles of the principal maxima of the diffraction intensity: The angle of the n th order principal diffraction maximum, θ_n , is given, in terms of the momentum P_y , by $P_y = P \sin \theta_n$. In a similar way, $P_y' = P' \sin \theta'$ determines the angle of incidence of the beam in the (x, y) plane perpendicular to each grating bar. Equations (10) and (11) then yield

$$\sin \theta_n = \left(1 - \frac{E_{\gamma} - E_{\gamma'}}{P'^2/2M}\right)^{-1/2} \left[\sin \theta' + n \frac{2\pi\hbar}{P'd}\right]. \quad (12)$$

For elastic ($E_{\gamma} = E_{\gamma'}$) diffraction this reproduces the well known formula from wave optics. For inelastic ($E_{\gamma} \neq E_{\gamma'}$) diffraction θ_0 is shifted to a larger (smaller) angle in the case of excitation (de-excitation) and the spacing of the diffraction maxima is increased (decreased). We note that equation (12) only contains the (de)excitation energy $E_{\gamma} - E_{\gamma'}$ but no further properties of the bound state wave functions. A physical interpretation of equation (12), in terms of refraction of molecular beams, was given in reference [11]. The break-up of a dimer leads to diffuse scattering angles of the fragments and will not be considered further in this article.

An experimental molecular beam exhibits a finite divergence which leads to a broadening of the diffraction maxima. The intensity of a diffraction order is usually obtained from the area under the corresponding peak. With this averaging procedure the diffraction intensities become independent of the beam properties as long as the peaks are resolved. The diffraction intensity of the n th order principal maximum for a transition between the bound states $\phi_{\gamma'}$ and ϕ_{γ} is then determined, in terms of the S matrix (3), through

$$I_n^{\gamma\gamma'} \propto \int_{C_n} d^3P \left| \int d^3P' \psi(\mathbf{P}') \langle \mathbf{P}, \phi_{\gamma} | S | \mathbf{P}', \phi_{\gamma'} \rangle \right|^2. \quad (13)$$

Here the momentum distribution $|\psi(\mathbf{P}')|^2$ accounts for the beam divergence and C_n denotes a small cone centered about the n th order principal diffraction maximum. The integration over the cone determines the area under the peak.

To resolve the diffraction orders $\psi(\mathbf{P}')$ should be sharply peaked about an average momentum $\overline{\mathbf{P}'}$ which defines the incident direction as well as the mean velocity of the beam of dimers. Under the assumption that the diffraction orders are resolved equations (3), (8) and (13) yield

$$I_n^{\gamma\gamma'} \propto \left| \frac{1}{d} \int_{-\frac{d}{2}}^{\frac{d}{2}} dY \exp(-i2\pi nY/d) \tau_{\gamma\gamma'}^{\text{dim}}(\overline{P}'_x, \overline{P}'_y; Y) \right|^2, \quad (14)$$

where the integral extends only over one period of the grating. The intensities of the diffraction peaks are thus determined by the properties of the transmission function $\tau_{\gamma\gamma'}^{\text{dim}}$.

4. Examples: Diffraction of $(D_2)_2$ and H_2D_2

We will now apply the above results to the van der Waals dimers $(D_2)_2$ and H_2D_2 . To an excellent approximation the dimer binding potential V remains unchanged under isotopic substitution. The different small reduced masses of $(D_2)_2$ and H_2D_2 , however, lead to pronounced isotope shifts in their bound state spectra. The binding energies of both species are of the order of only a few hundred μeV . Along with $(H_2)_2$ these dimers were extensively studied, both theoretically and experimentally, after finding evidence of $(H_2)_2$ in astrophysical planetary spectra. According to their total nuclear spin one distinguishes between the ortho (o) and para (p) modifications of H_2 and D_2 . All of them may combine to form dimers, leading to a rich infrared fluorescence spectrum (see, e.g., references [15, 16, 17, 18], and references [23, 24] for a recent overview of binding potentials).

To facilitate the following discussion we will assume that, by passing the gas through a catalytic converter or by a similar experimental technique, the molecular beam contains only o- D_2 and p- H_2 . Both molecules exhibit only even rotational angular momentum quantum numbers j . Furthermore, we shall assume that the nozzle temperature of the beam apparatus is sufficiently low that the majority of the D_2 and H_2 molecules are in their rotational ground states $j = 0$ [25].

To determine the dimer transmission function from equation (9) we first have to calculate the bound state wave functions $\phi_\gamma(\mathbf{r})$ that describe the dimers $(D_2)_2$ and H_2D_2 . To this end we have chosen the semi-empirical potential $V(\mathbf{r})$ by Buck *et al* [26] which is given in analytic form. Its anisotropic contributions will be neglected as we assume the constituents to be mostly in spherically symmetric $j = 0$ states. Then, as usual, the stationary two body Schrödinger equation can be expanded in terms of spherical harmonics $Y_l^m(\vartheta, \varphi)$ and one only needs to determine the radial part. A numerical integration of the radial equation yields four rotational bound states for (o- D_2) $_2$ and three for p- H_2 -o- D_2 , all belonging to the lowest vibrational mode. As higher vibrational modes are unbound the radial bound state wave functions $R_l(r)$, as depicted in figure 2, are determined solely by their end-over-end rotational quantum number l . Within our approximations the binding energies of (o- D_2) $_2$ are in agreement with reference [16].

The integration over the relative coordinate $\mathbf{r} = (x, y, z)$ in the dimer transmission function (9) can be performed most conveniently in spherical coordinates ($\int d^3r = \int_0^\infty r^2 dr \int_0^{2\pi} d\varphi \int_0^\pi \sin\vartheta d\vartheta$). By choosing $y = r \cos\vartheta$ the angular integration over φ becomes trivial and the substitution $\alpha = \cos\vartheta$ yields

$$\begin{aligned} \tau_{lm'l'm'}^{\text{dim}}(P'_x, P'_y; Y) &= \delta_{mm'} \sqrt{2l+1} \sqrt{2l'+1} \int_0^\infty r^2 dr R_l(r) R_{l'}(r) \int_{-1}^1 d\alpha \Pi_{ll'}^{m'}(\alpha) \\ &\times \tau_1^{\text{PP}} \left(\frac{m_1}{M} P'_x, \frac{m_1}{M} P'_y; Y + \frac{m_2}{M} \alpha r \right) \tau_2^{\text{PP}} \left(\frac{m_2}{M} P'_x, \frac{m_2}{M} P'_y; Y - \frac{m_1}{M} \alpha r \right). \end{aligned} \quad (15)$$

Here the function $\Pi_{ll'}^{m'}(\alpha)$ has been introduced as

$$\Pi_{ll'}^{m'}(\alpha) = \frac{1}{2} \sqrt{\frac{(l-|m'|)! (l'-|m'|)!}{(l+|m'|)! (l'+|m'|)!}} P_l^{|m'|}(\alpha) P_{l'}^{|m'|}(\alpha), \quad (16)$$

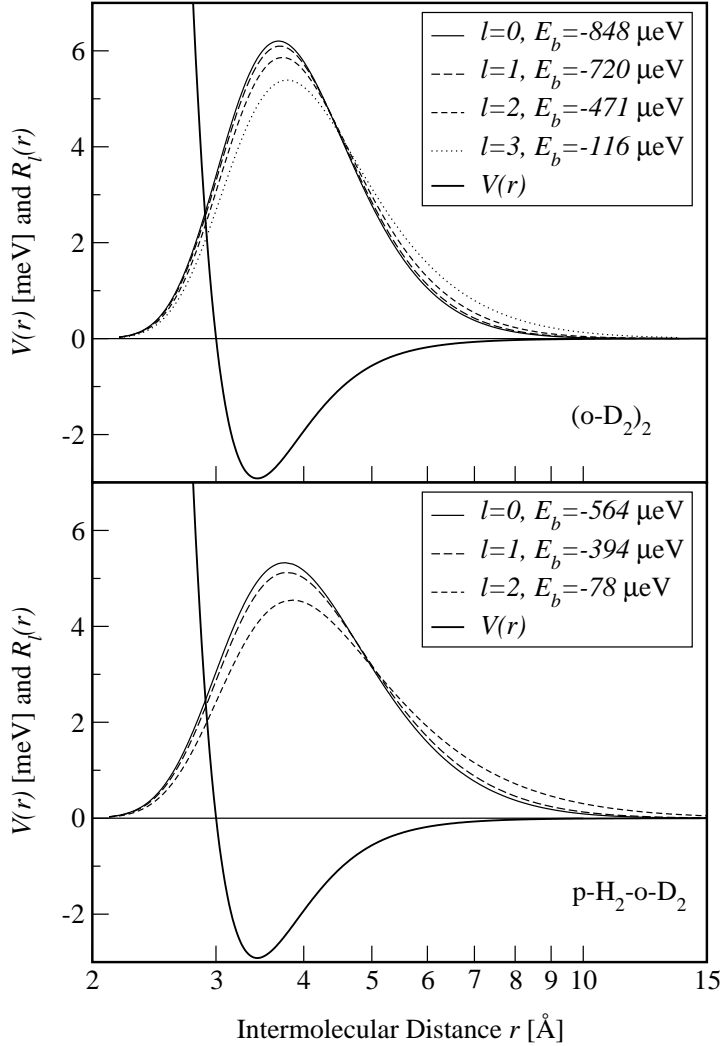


Figure 2. The radial wave functions $R_l(r)$ of $(o-D_2)_2$ (top) and $p-H_2-o-D_2$ (bottom), where l denotes the end-over-end rotational quantum number. The corresponding binding energies are given in the legend. All bound states belong to the lowest vibrational modes. Higher vibrational modes are unbound for both species. The radial coordinate is given on a logarithmic scale. The ordinates refer to the binding potential $V(r)$ from reference [26] which is shown for comparison.

where P_l^m are the associated Legendre polynomials. $\Pi_{ll'}^{m'}(\alpha)$ is symmetric in the indices l and l' . For identical constituents the symmetry properties of the associated Legendre polynomials with respect to reflections at the origin imply a parity conservation selection rule for the inelastic diffraction intensity:

$$l' + l = \text{even}. \quad (17)$$

This selection rule can be obtained from equation (15) when one inserts $m_1 = m_2 = M/2$ but may also be derived directly from general symmetry properties of the Hamiltonian (1).

We assume the dimer bound states in the incident beam to be populated in

accordance with the thermal equilibrium weight factors $p_{l'} = (2l' + 1) \exp(-E_{l'}/k_B T_b)$ where T_b is the translational beam temperature and k_B is the Boltzmann constant. Inserting equation (15) into equation (14) and summing over m' we find that the n th order diffraction intensity for a transition $l' \rightarrow l$ is given by

$$I_n^{ll'} \propto (2l + 1) p_{l'} \sum_{m'} \left| \frac{1}{d} \int_{-\frac{d}{2}}^{\frac{d}{2}} dY \exp(-i2\pi nY/d) \int_0^\infty r^2 dr R_l(r) R_{l'}(r) \int_{-1}^1 d\alpha \Pi_{ll'}^{m'}(\alpha) \right. \\ \left. \times \tau_1^{\text{PP}} \left(\frac{m_1}{M} P'_x, \frac{m_1}{M} P'_y; Y + \frac{m_2}{M} \alpha r \right) \tau_2^{\text{PP}} \left(\frac{m_2}{M} P'_x, \frac{m_2}{M} P'_y; Y - \frac{m_1}{M} \alpha r \right) \right|^2, \quad (18)$$

where, due to the factor $\delta_{mm'}$ in equation (15), only the orientation quantum numbers m' between $-\min(l, l')$ and $\min(l, l')$ contribute to the sum.

By considering D_2 and H_2 as point particles we have neglected transitions between rotational states of the constituents. Due to their small moments of inertia, however, the $j=0 \rightarrow 2$ transition energies are comparatively large, i.e. 22 meV for o- D_2 and 44 meV for p- H_2 [25]. By keeping the kinetic energy in the beam below these thresholds excitation of higher j states can, therefore, be ruled out.

The diffraction patterns in the following two subsections (figures 3 and 4) were calculated with experimentally realizable parameters in mind. The mean beam velocity was chosen as $v' = \overline{P'}/M = 500 \text{ ms}^{-1}$ with a velocity spread of $\Delta v'/v' = 8\%$ [27, 6]. This corresponds to a kinetic energy of 5.2 meV for D_2 (2.6 meV for H_2), and a translational beam temperature of $T_b \approx 0.4 \text{ K}$ in a pure D_2 -beam. We have considered diffraction from a typical silicon nitride grating, as characterized experimentally in reference [6], with a grating period of $d = 100 \text{ nm}$, a slit width of $s = 60 \text{ nm}$, and a wedge angle of the grating bars of $\beta = 5^\circ$. The attractive van der Waals interaction between the grating and the constituents is accounted for in the point particle transmission functions. Its C_3 coefficient (see Appendix) has been determined experimentally for silicon nitride and D_2 as $C_3 = 0.32 \text{ meV nm}^3$ [6]. We are not aware of a corresponding experimental value for H_2 which we therefore estimated: According to Hoinkes' empirical rule [28, 6, 7] C_3 is, quite generally, proportional to the static electric dipole polarizability of the atom or molecule. The polarizabilities of H_2 and D_2 differ by about 1% only. We thus assumed the same C_3 for both D_2 and H_2 .

In a typical experiment the diffraction maxima are broadened due to the beam divergence and the width of the detector slit. The finite velocity spread of a beam leads to an additional broadening which increases with the diffraction order n . These mechanisms are all specific to the experimental setup. We, therefore, use an empirical model to include the broadening. Previous experimental studies [6, 9] have shown that the maxima can be represented, to an excellent approximation, by Gaussians of the form

$$\frac{I}{\sqrt{\pi} w_n} \exp\left(-(\theta - \theta_n)^2/w_n^2\right)$$

whose widths w_n depend on the diffraction order n as

$$w_n = w_0 \sqrt{1 + \left(\frac{\Delta w}{w_0} n\right)^2}.$$

Here w_0 is the angular width of the zeroth order diffraction maximum and Δw accounts for the velocity spread. For the beams in the present applications we have chosen $w_0 = 3 \times 10^{-3}$ degrees and $\Delta w = 7 \times 10^{-4}$ degrees. Each diffraction maximum is thus represented by a Gaussian of this kind with an area I given by equation (18). The angle of incidence θ' was chosen in such a way that the zeroth order principal diffraction maxima of all inelastic transitions do not overlap with the zeroth order elastic peak.

4.1. Diffraction of $(o-D_2)_2$

In the case of $(o-D_2)_2$ both constituents are identical and the selection rule (17) applies. Table 1 shows the allowed transitions and the corresponding excitation energies. Due to

Table 1. Allowed excitations $l' \rightarrow l$ for $(o-D_2)_2$ and transition energies for the dimer binding potential from reference [26]. Also allowed are the reverse processes (de-excitation) with negative transition energies.

$l' \rightarrow l$	$E_l - E_{l'} [\mu\text{eV}]$
elastic ($l' = l$)	0
0 \rightarrow 2	377
1 \rightarrow 3	604

the low translational beam temperature of $T_b \approx 0.4$ K most dimers are in the rotational ground state $l' = 0$. The population of the $l' = 1$ state is only of the order of 7%, and the initial populations of higher excited states are negligible.

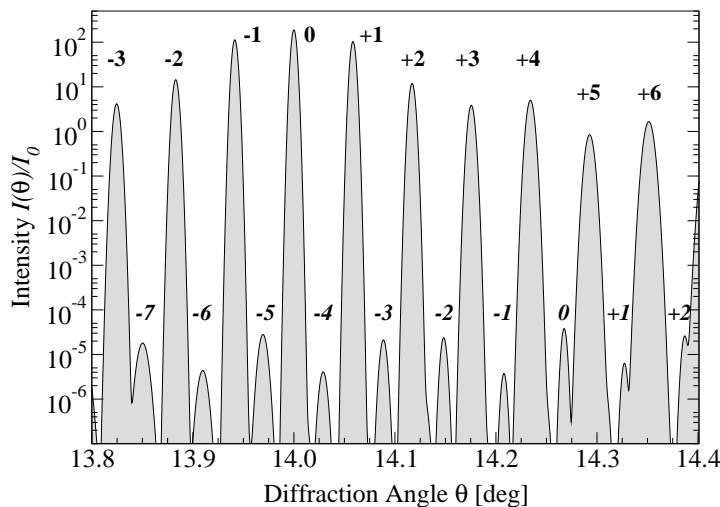


Figure 3. Diffraction pattern of a pure $(o-D_2)_2$ beam including all allowed transitions $l' \rightarrow l$. The angle of incidence is $\theta' = 14^\circ$. The intense diffraction maxima are due to elastic scattering. The italic labels indicate the inelastic 0 \rightarrow 2 diffraction orders. Other inelastic transitions are masked or too weak to be resolved. The diffraction pattern is normalized to the total elastic zeroth order intensity $I_0 = I_0^{00} + I_0^{11} + I_0^{22} + I_0^{33}$.

Figure 3 shows a $(o\text{-D}_2)_2$ diffraction pattern with an angle of incidence of $\theta' = 14^\circ$. The intense maxima correspond to elastic scattering whereas the weak maxima result from the inelastic $0 \rightarrow 2$ transition. The even weaker $1 \rightarrow 3$ maxima are too close to the elastic diffraction peaks to be resolved. According to equation (12) the spacing of the $0 \rightarrow 2$ maxima and the shift of the zeroth order with respect to the incident beam direction determine the excitation energy $E_2 - E_0 = 377 \mu\text{eV}$. The hierarchy of the inelastic maxima depends on the specific interaction with the grating bars.

4.2. Diffraction of $p\text{-H}_2\text{-}o\text{-D}_2$

In the case of $p\text{-H}_2\text{-}o\text{-D}_2$ the selection rule (17) does not apply, allowing all transitions between the three bound states. Their excitation energies are shown in table 2. Again,

Table 2. Allowed excitations $l' \rightarrow l$ for $p\text{-H}_2\text{-}o\text{-D}_2$ and transition energies for the dimer binding potential from reference [26]. Also allowed are the reverse processes (de-excitation) with negative transition energies.

$l' \rightarrow l$	$E_l - E_{l'} [\mu\text{eV}]$
elastic ($l' = l$)	0
$0 \rightarrow 1$	170
$0 \rightarrow 2$	486
$1 \rightarrow 2$	316

most dimers are in the rotational ground state $l' = 0$. About 2% of the dimers are in the $l' = 1$ state, and the initial population of the $l' = 2$ state is negligible.

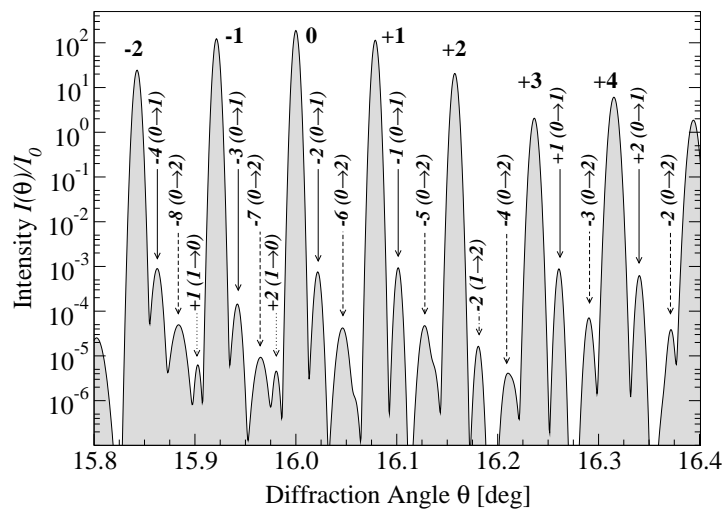


Figure 4. Diffraction pattern of a pure $p\text{-H}_2\text{-}o\text{-D}_2$ beam including all allowed transitions. The angle of incidence is $\theta' = 16^\circ$. The intense diffraction maxima are due to elastic transitions. The italic labels indicate the resolvable inelastic diffraction orders. The diffraction pattern is normalized to the total elastic zeroth order intensity $I_0 = I_0^{00} + I_0^{11} + I_0^{22}$.

Figure 4 shows a p-H₂-o-D₂ diffraction pattern with an angle of incidence of $\theta' = 16^\circ$. Besides the intense elastic maxima the inelastic transitions 0→1 and 0→2 are resolved. Their spacings determine the transition energies of $E_1 - E_0 = 170\mu\text{eV}$ and $E_2 - E_0 = 486\mu\text{eV}$, respectively. The 0→1 diffraction maxima are, in general, about an order of magnitude more intense than the 0→2 ones. It is interesting to note, however, that the 0→1 zeroth order is strongly suppressed because the point particle transmission functions of H₂ and D₂ are almost equal and almost symmetric. The zeroth order vanishes exactly in the hypothetical limit that the van der Waals interaction of the constituents with the grating vanishes. Also visible, but weaker because of the small initial $l' = 1$ population, are some maxima of 1→0 and 1→2 transitions.

5. Conclusions

We have shown in this article how inelastic diffraction from a transmission grating may be used to study energy spectra of very weakly bound two body clusters. The transition energies are determined by angular shifts of the inelastic diffraction peaks in comparison to the strong elastic peaks. The emergence of these peaks is implied by the periodicity of the grating. We have determined their relative intensities from a quantum mechanical few body scattering approach for the examples of the van der Waals dimers (D₂)₂ and H₂D₂.

For these realistic examples the angles of the inelastic diffraction peaks can be resolved in present day experiments while their small intensities would require an additional gain in sensitivity. This gain may be achieved, for instance, by increasing the detection efficiency and, thereby, keeping the background detection rate at a constant level.

Given a suitable detection efficiency the inelastic diffraction technique described in this article should be applicable also to those very weakly bound clusters that are not easily excited by laser light. A prominent example of this kind, the helium trimer, was discussed in reference [11]. Inelastic diffraction from a transmission grating may also be used to separate beams of clusters in particular internal states from the incoming beam.

Acknowledgments

We would like to thank R. Brühl, G. C. Hegerfeldt and J. P. Toennies for interesting discussions. This research was supported by the Alexander von Humboldt Foundation and the United Kingdom EPSRC.

Appendix. The Point Particle Transmission Function

In reference [21] the point particle transmission function was derived in terms of an exact scattering solution of the two-dimensional stationary Schrödinger equation as (cf. figure

A1):

$$\tau^{\text{PP}}(p'_x, p'_y; y) = \exp(-ip'_y y/\hbar)\varphi(0, y).$$

Here this scattering solution $\varphi(x, y)$ assumes, at large distances from the grating, the asymptotic form of a coherent superposition of the incoming plane wave $\exp[i(p'_x x + p'_y y)/\hbar]$ and an outgoing cylindrical wave. In this appendix we will explain the methods we have used to determine $\tau^{\text{PP}}(y)$. We shall focus on off normal incidence of the incoming beam ($\theta' \neq 0$) as the case of normal incidence on the transmission grating was discussed in detail in references [21, 6]. The coordinates as well as the typical trapezoidal shape of the grating bars [6] are depicted schematically in figure A1. As the grating bars are assumed to reflect those atoms that touch the bar walls the wave function $\varphi(x, y)$ vanishes at the surface of the bars. This implies $\tau^{\text{PP}}(y) = 0$ for the coordinates y at the rear of a grating bar. The point particle transmission function $\tau^{\text{PP}}(y)$ in the slits can be determined in accordance with the standard eikonal approximation [29]: When, at off normal incidence, θ' exceeds the wedge angle β a portion $t(\tan \theta' - \tan \beta)$ of each slit is shaded by the adjacent grating bar (see figure A1). In this case $\tau^{\text{PP}}(y)$ also vanishes in the shadow region. For the coordinates y inside the remaining open fraction of a slit the

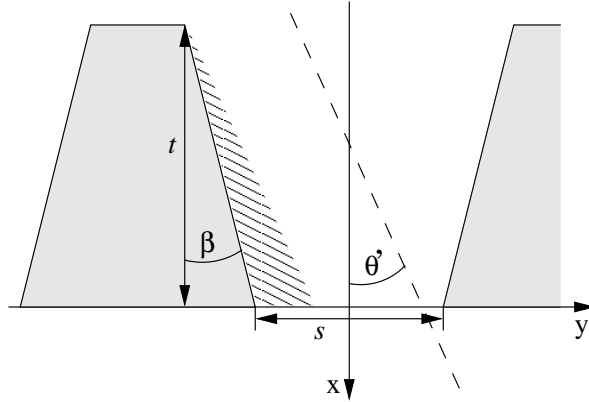


Figure A1. The trapezoidal shape of the grating bars with thickness t and wedge angle β , and the direction of the incident beam (dashed line). For $\theta' > \beta$ a portion of the slit is shadowed (hatched region).

point particle transmission function assumes the form $\tau^{\text{PP}}(y) = \exp[i\Phi(y)]$. The phase shift $\Phi(y)$ accounts for the attractive van der Waals interaction between the atom or molecule and the grating bars. It is determined by

$$\Phi(y) = -\frac{1}{\hbar v'} \int du W_{\text{att}}(u), \quad (\text{A.1})$$

where $v' = \sqrt{p_x'^2 + p_y'^2}/m$ is the velocity of the incoming atom or molecule and the integration is performed along a straight line in the direction of the beam (dashed line in figure A1).

The long range van der Waals potential between a pair of atoms (or molecules) separated by a distance R is proportional to $-R^{-6}$. To determine the functional form of

the attractive interaction between an atom or molecule and the grating one may use a pairwise summation of the interactions between the probe particle and the constituents of the solid. For an idealized flat surface, i.e. when the solid covers the half space, the pairwise summation implies the well known functional form $W_{\text{att}} = -C_3/L^3$, where L denotes the distance between the probe particle and the surface. The coefficient C_3 depends on the static electric dipole polarizability of the atom or molecule and the material of the solid [6, 28]. For D_2 and a silicon nitride grating C_3 is known experimentally [6]. For H_2 C_3 has been estimated as explained in Section 4.

For a grating bar with the geometrical form in figure A1 the attractive interaction W_{att} does not assume a simple form. By interchanging the pairwise summation with the integral in equation (A.1), however, the phase shift may be determined analytically. Numerical studies have shown that only those bars contribute significantly to W_{att} that confine the actual slit. At off normal incidence with $\theta' > \beta$ the phase shift is then given by

$$\Phi(y) = \frac{C_3}{2\hbar v'(\cos \theta')^4} \left[\frac{\xi_{11}^{-2} - \xi_{12}^{-2}}{\tan \theta' + \tan \beta} + \frac{\xi_{21}^{-2} - \xi_{22}^{-2}}{\tan \theta' - \tan \beta} \right], \quad (\text{A.2})$$

where $\xi_{11} = s/2 - y$, $\xi_{12} = s/2 + t(\tan \beta + \tan \theta') - y$, $\xi_{21} = s/2 + t(\tan \beta - \tan \theta') + y$ and $\xi_{22} = s/2 + y$.

References

- [1] Leavitt J A and Bills F A 1969 *Am. J. Phys.* **37** 905
- [2] Keith D W, Schattenburg M L, Smith H I and Pritchard D E 1988 *Phys. Rev. Lett.* **61** 1580
- [3] Carnal O and Mlynek J 1991 *Phys. Rev. Lett.* **66** 2689
- [4] Schöllkopf W and Toennies J P 1994 *Science* **266** 1345
- [5] Chapman M S, Ekstrom C R, Hammond T D, Rubenstein R A, Schmiedmayer J, Wehinger S and Pritchard D E 1995 *Phys. Rev. Lett.* **74** 4783
- [6] Grisenti R E, Schöllkopf W, Toennies J P, Hegerfeldt G C and Köhler T 1999 *Phys. Rev. Lett.* **83** 1755
- [7] Brühl R, Fouquet P, Grisenti R E, Toennies J P, Hegerfeldt G C, Köhler T, Stoll M and Walter C 2002 *Europhys. Lett.* **59** 357
- [8] Arndt M, Nairz O, Vos-Andreae J, Keller C, van der Zouw G and Zeilinger A 1999 *Nature (London)* **401** 680
- [9] Grisenti R E, Schöllkopf W, Toennies J P, Hegerfeldt G C, Köhler T and Stoll M 2000 *Phys. Rev. Lett.* **85** 2284
- [10] Whaley K B, Yu C, Hogg C S, Light J C and Sibener S J 1985 *J. Chem. Phys.* **83** 4235
- [11] Hegerfeldt G C and Köhler T 2000 *Phys. Rev. Lett.* **84** 3215
- [12] Esry B D, Lin C D and Greene C H 1996 *Phys. Rev. A* **54** 394
- [13] Boustimi M, Baudon J, Ducloy M, Reinhardt J, Perales F, Mainos C, Bocvarski V and Robert J 2001 *Eur. Phys. J. D* **17** 141
- [14] Boustimi M, Baudon J, Pirani F, Ducloy M, Reinhardt J, Perales F, Mainos C, Bocvarski V and Robert J 2001 *Europhys. Lett.* **56** 644
- [15] Danby G 1983 *J. Phys. B* **16** 3411
- [16] Danby G 1989 *J. Phys. B* **22** 1785
- [17] McKellar A R W and Welsh H L 1974 *Can. J. Phys.* **52** 1082
- [18] McKellar A R W 1990 *J. Chem. Phys.* **92** 3261
- [19] Hegerfeldt G C and Köhler T 1998 *Phys. Rev. A* **57** 2021

- [20] Alt E O, Grassberger P and Sandhas W 1967 *Nucl. Phys. B* **2** 167
- [21] Hegerfeldt G C and Köhler T 2000 *Phys. Rev. A* **61** 23606
- [22] Born M and Wolf E 1959 *Principles of Optics* (Pergamon Press)
- [23] Schaefer J 1994 *Astron. Astrophys.* **284** 1015
- [24] Diep P and Johnson J K 2000 *J. Chem. Phys.* **112** 4465
- [25] Kern K, David R and Comsa G 1985 *J. Chem. Phys.* **82** 5673
- [26] Norman M J, Watts R O and Buck U 1984 *J. Chem. Phys.* **81** 3500
- [27] Winkelmann K 1979 in *Rarefied Gas Dynamics*, ed. R Camparque (CEA, Paris) vol. 2 p. 899
- [28] Hoinkes H 1980 *Rev. Mod. Phys.* **52** 933
- [29] Joachain C J 1975 *Quantum Collision Theory* (North-Holland Physics Publishing)